D. CHICET[1], S. TOMA[1*], R. HARAGA[1], C. BEJINARIU[1]

COMPARATIVE ROLLING CONTACT BEHAVIOR OF TWO APS COATINGS WITH DIFFERENT MATRIX

In this study we analyzed the rolling contact fatigue behavior of two types of coatings made by thermal coating, by the method of atmospheric plasma spraying (APS) from two commercially available powders: Ni5Al5Mo and $Al_2O_3 - 13\ TiO_2$. The contact fatigue behavior was studied on an installation specially designed. The specimens were tested for 54 hours (at 1380 rpm), at a load of 944 N. For both types of coatings, the appearance of a wear path was observed, much more obvious in the case of the Ni matrix layer, also confirmed by profilometry. The mechanism of the wear phenomenon was predominantly of plastic deformation type (the material was pushed towards the edges of the wear path) in the case of NiAlMo coating. In the case of ceramic coating, the wear path width was very small (300-450 μm), with very few changes at the surface level of the coating, which recommends this type of material for applications that require wear resistance to rolling.

Keyword: Rolling Contact Fatigue; Atmospheric Plasma Spray; Wear Path Microstructure

1. Introduction

Plasma spray coatings have become increasingly used in last decades to improve the life of key components operating in hostile environments [1]. These coatings behave as the "first line of defense" against the usual mechanisms of surface degradation, such as: corrosion, oxidation, wear of any kind (abrasive, adhesive), defects caused by overheating and so on. Obtaining a high-performance coating on a particular part made of an alloy / metal with high mechanical strength, offers an attractive way to combine the surface requirements with those for the part itself, for almost any conceivable application. This concept of surface modification plays an important role in reducing the frequency of damage to components produced at relatively high costs [2-5].

Plasma jet spraying was initially developed in order to make coatings from ceramic materials, being still the most important process for making these layers [6,7]. With this process, a wide range of materials can be sprayed, from metallic to plastic (even polymeric coatings can be made today), the versatility of the process being given by the wide range of materials that can be used, the high limits of temperature that can be reached in the plasma jet, by the possibility of varying the spray distance, the powder flow used and so on [8-10].

One of the main causes of failure of the components involved in rolling and sliding-rolling contacts (eg bearings, gears, cams, eccentric mechanisms) is contact fatigue [11,12]. This phenomenon can be defined as the mechanism for generating and propagating cracks, caused by cyclic high-stress field in a small volume of material specific to concentrated tribo-contacts, which can ultimately lead to micro-cracks, pitting, and spalling [13].

The production of wear by contact fatigue is directly related to the microscopic defects of the superficial layer of the material (the existence of inclusions or gaps) and surface defects caused by mechanical processing (scratches, microcracks, stains, potholes) or microdefects from the wear process, adhesive or abrasive type [14,15].

We can summarize the interconditioning parameters of contact fatigue in the case of a rolling and sliding contact depending on:

– surface quality: microdefects; microcracks; material detachments; porosity; pitting; flaking; large detachments (spalling); plastic flows;
– the appearance, from the depth to the surface, of the microdefects, microcracks; cracks;
– material properties: modulus of elasticity; hardness; fatigue resistance;
– lubricant properties: viscosity; degree of contamination;
– load applied to the surface: load size; the meaning of application; mode of variation.

[1] GHEORGHE ASACHI TECHNICAL UNIVERSITY OF IASI, DEPARTMENT OF MATERIALS SCIENCE AND ENGINEERING, BLVD. MANGERON, NO. 41, 700050, IASI, ROMANIA.

* Corresponding author: stefan-lucian.toma@academic.tuiasi.ro

In this study we analyzed the contact fatigue behavior of two types of coatings made by thermal coating, by the APS method, from commercial available powders: a metallic powder with Ni matrix (Ni5Al5Mo) and a ceramic powder based on Al_2O_3 (Al_2O_3 – 13 TiO_2). The samples were tested for 54 hours (at 1380 rpm), at a load of 944 N (calculated for the case of the hertzian elastic point contact), on a test rig specially designed for rolling contact tests.

2. Experiment

2.1. Materials and methods used for samples

In the present paper, the research was performed on 2 types of coatings produced by plasma spray, using the following powders:

A. A powder from the category of Ni based materials – nickel-aluminum-molybdenum mixture, with the nominal composition Ni 5Al 5Mo (see Fig. 1), with spheroidal shape particles and 2-15 μm dimension range. The coatings thus obtained have high density, are resistant to oxidation and corrosion at high temperature. The addition of Mo ensures good wear and erosion resistance and a low shrinkage coef-

ficient [16]. The samples obtained with this type of powder were hereinafter referred to as P1.

B. A powder of the ceramics class – aluminum oxide mixed with titanium oxide, with the nominal composition Al_2O_3 – 13 TiO_2 (see Fig. 2) with polygonal shape particles and 5-20 μm dimension range. These materials are used for coatings subjected to abrasive and slip wear, have oxidation resistance at working temperatures of about 550°C and have a good behavior in alkaline or acidic environments. The samples obtained with this type of powder were hereinafter referred to as P2.

Steel rings for bearings (Øext = 47 mm, Øint = 27 mm, thickness g = 4 mm), 100Cr6 grade, were used as coating support, with the following chemical composition, according to ISO 683-17: 0.93-1.05% C, 0.15 0.35% Si, 0.25-0.45% Mn, 1.35-1.6% Cr, max. 0.10 MB, max. 0.025% P, max. 0.015% S.

The first step in making the coatings was to prepare the substrate. First, the rings were sandblasted for texturing, using F20 type electrocorundum as abrasive material, reaching a roughness before coating Ra = 0.50 μm, and later they were cleaned in the ultrasonic bath using a degreasing solution of trichlorethylene.

The coating of the samples was performed with the help of a plasma spray facility SPRAYWIZARD 9MCE type (Sulzer
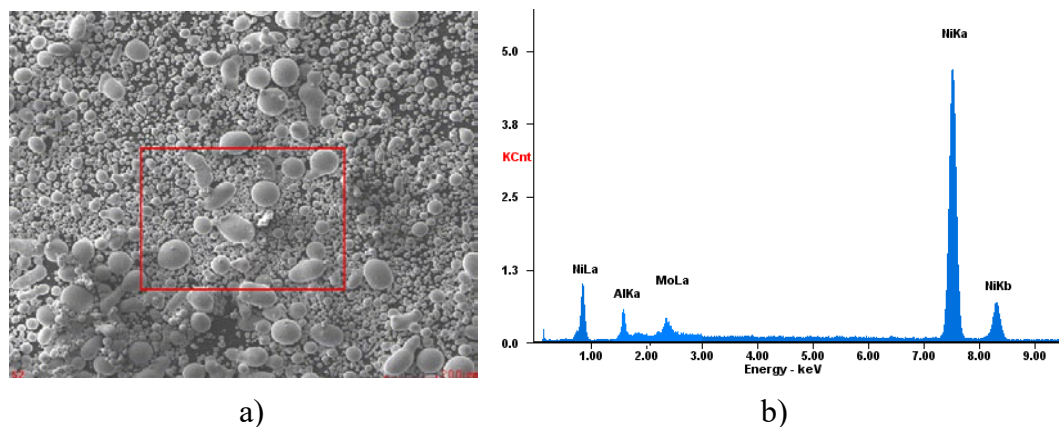

a)   b)

Fig. 1. Ni5Al5Mo powder: a) secondary electrons (SE) image; b) Energy-dispersive X-ray spectroscopy (EDS) spectrum
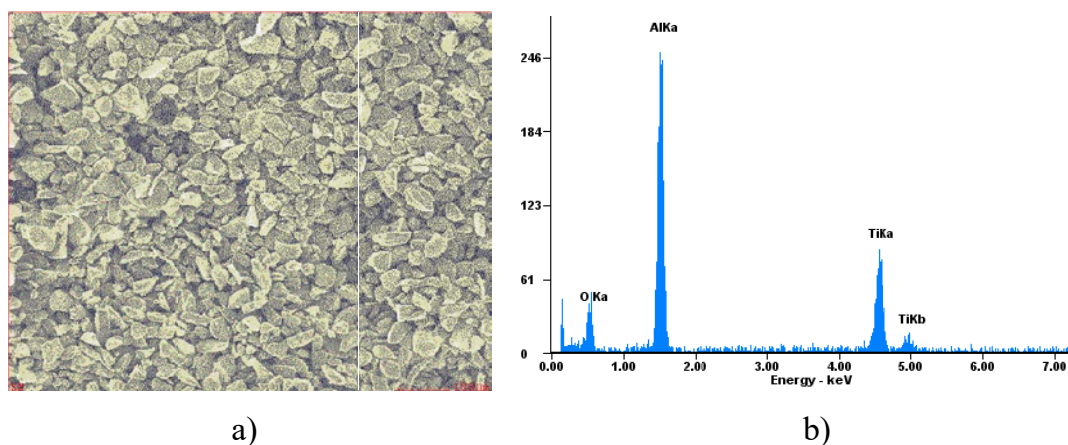

a)   b)

Fig. 2. Al_2O_3 – 13 TiO_2 powder: a) (SE) image; b) EDS spectrum

Metco, 2008), equipped with a 9MBM spray gun. The samples were fixed on the rotating table of the equipment, to have a fixed controllable position during the spraying process, being coupled in batches of three, as can be seen in Fig. 3.
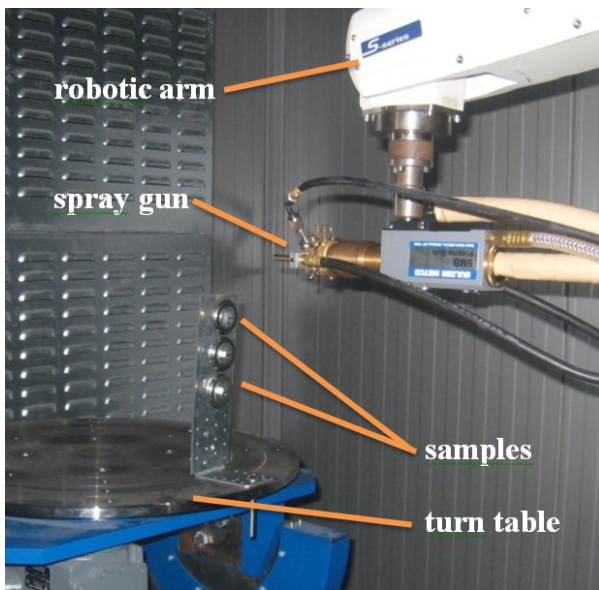

Fig. 3. Aspect of the plasma spray process

The movement of the spray gun mounted on the robotic arm was controlled by a program made with the help of COSIROP software and consisted of moving at a constant speed on the horizontal lines of a chosen rectangular field so that the three rings are evenly covered during the spraying process. The process parameters are presented in TABLE 1.

TABLE 1

Atmospheric plasma spray process parameters

Powder	Ni 5Al 5Mo	$Al_2O_3 - 13\ TiO_2$
Ar flow (l/min)	46	46
H_2 flow (l/min)	13.5	13.5
Ar flow – as carrier gas (l/min)	45	45
Voltage (V)	60	60
Intensity (A)	600	600
Spray distance (mm)	120	120

2.2. Samples characterisation

Several methods and techniques were used to analyze the characteristics of the coatings:

1. Images of secondary electrons obtained with the help of the Quanta 200 3D electron microscope (FEI, Holland, 2008), for the analysis of powders being used the High Vacuum (HV) module (the powders were attached to the specific support with a special carbon tape), and for the analysis of coatings were used both the HV module and the Low Vacuum (LV) module with the LFD (Large Field) Detector

at working pressures between 30-60 Pa. The electron beam acceleration voltage used was 30 kV, and the spray distance varied between 12-19 mm. In addition, semi-quantitative elementary chemical analyzes (EDS type) were performed using the analysis module produced by EDAX-AMETEK (Holland, 2008), attached to the same scanning electron microscope.

2. The X – ray analysis, necessary for the comparative observation of the existing phases and constituents both in the plasma sprayied coatings and in the powders, was conducted with the help of the X'PERT PRO MRD diffractometer equipped with a Cu anode with λ = 1.54 Å, open eulerian cradle samples support and working angle 2θ = 20-90º.

3. Surface roughness measurements and profilometry were performed using the Form Talysurf Intra system, produced by Taylor Hobson LEICESTER, ENGLAND.

2.3. Materials and methods used for the rolling contact wear tests

The rolling contact fatigue tests were performed on a specially designed and patented test rig, with the purpose of testing two specimens simultaneously (no. 60919/1985), at the Department of Machine Parts and Mechatronics of the Faculty of Mechanics – Technical University "Gh. Asachi "Iaşi [17]. It consists of a tank A (see Fig. 4) in which a spacer is mounted, on which two axial bearing rings are fixed, together with two cages with rolling bodies and two conical rings for fixing the two flat specimens. The component parts of the fatigue test rig, according to Fig. 4, are the following: 1 – electric motor; 2 – mechanical coupling; 3 – main shaft; 4, 5 – bearings; 6 – weight loading system; 7 – loading lever; 8 – fork; 10 – adjusting screw; 11 – locking screw; 12 – piston; 20 – uprights. The axial load is taken over by the machine frame by means of a spherical surface, so that the main shaft has no load at all. In this system, the movement is transmitted from the electric motor 1, fixed on the frame with screws, by means of a coupling with bolts 2. The rotational movement is transmitted to the main shaft 3, supported on two radial ball bearings 4 and 5, type 6211-2RS (encapsulated bearings are used due to the lubrication difficulties of the bearings mounted in the housing).

The axial loading is performed by means of the loading system (6) composed of a series of weights mounted on a shaft, being amplified and transmitted by a system of levers (7), with the transmission ratio i = 26, to the tank A of the machine in which the test specimens are mounted.

The loading system consists of a plate rod with a weight of 1,740 kg, on which a series of weights of 1 kg can be mounted, depending on needs. The plate rod is connected to the arm (9) of the lever system by a movable joint to take over the oscillating movements of the system (6), thus ensuring a simple, quiet and efficient loading solution.

From the operating lever 9, through the fork 8, the loading force is transmitted to the loading lever 7, which ensures by
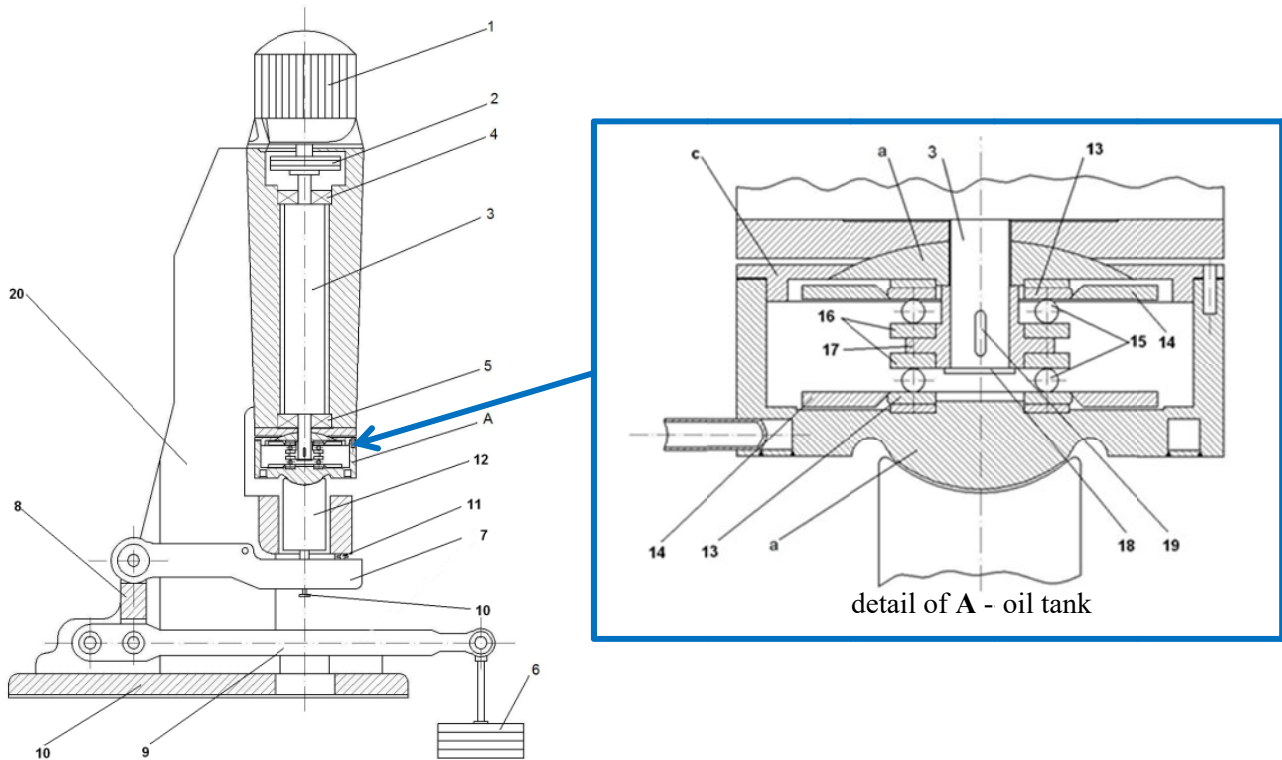
Fig. 4. Rolling fatigue test rig with an oil tank A, in which the test specimens are mounted, presented in detailed view [17]

means of the adjusting screw 10 the transmission of the force to the piston 12 and then to the tank. In order to ensure a strictly axial force transmission, the screw 10 and the piston 12 are provided with a conjugate outer and inner spherical surface, respectively.

In order to reduce the friction in the bearings and to increase the sensitivity of the loading system, a constructive solution was adopted based on the mounting in the lever joints of two radial bearings with cylindrical rollers type NI 210 E.

The tank A is placed on a spherical surface, as presented in Fig. 4. From the tank A, the load is transmitted to the samples 13 (centered on the bolts and fixed by means of two rings 14) with the help of two axial ball bearing cages, on the spacer 17 supported by the washer 18. Since the spacer bushing is sliding on the shaft 3, the load is transmitted uniformly to the two samples 13.

One of the samples is fixed on the lid of the tank A which has an outer spherical surface, conjugated to the inner spherical surface of the lid c. By means of these spherical surfaces the force is transmitted from the upper specimen to the housing and then to the gantries 20. These, together with the housing form the frame of the machine, executed as welded construction and stiffened with gussets.

Both the spherical surfaces of the caps and the spherical surfaces belonging to the tank and the piston are part of the same sphere in order to allow the tank to make a slight inclination to take up any deviations from coaxiality between the shaft, the bushing and the bearing rings.

The movement is taken up by the spacer bushing from the main shaft by means of a parallel wedge 19, symmetrically ar-

ranged and transmitted to the axial bearing rings 16, which in turn set the ball cages 15 in motion.

The flat samples replacing the second ring of the axial bearing are thus tested for contact fatigue. Lubrication is provided by filling the tank with oil, and cooling (if necessary).

In order to establish the loading force of the system during the rolling contact fatigue test, a series of initial data of the loading system were established, necessary to carry out the tests in good conditions:

– the multiplication factor of the system is i = 26;
– weight of the lever system Gsp = 500 N,
– the weight of the loading system (without other weights) is: Gsi = 944 N,
– the weight of the loading system (in case of using a standard additional weight of 1 kg) is: Gsi = 1199 N.

For the calculation of the loading force, it was taken into account that we have the case of a hertzian elastic point contact, in which one of the contact surfaces is a sphere and the other is flat, taking into account the rolling ball diameter d = $8 \cdot 0^{-3}$ m . The loading force was chosen according to the maximum contact stress generated during the operation of the test rig, a second variable being the thickness of the layer produced by atmospheric plasma spray [18]. Taking into account the existing variables, the calculations were performed using a Mathcad routine, by drawing the variation curves of the maximum contact stress σ_0 and the contact half-axis a, whose values are specified in TABLE 2.

Based on these calculations, the value Fa = 944 N was chosen as the load in the case of contact fatigue tests, for the load of the system being sufficient the own weight of the lever system.

TABLE 2

The values of contact stresses and semi-axes dimensions
for the samples

Calculated values / Load	P1		P2	
	σ_0 [Pa]	a [μm]	σ_0 [Pa]	a [μm]
500 [N]	$1.55\cdot10^9$	108.7	$1.61\cdot10^9$	106.9
944 [N]	$1.92\cdot10^9$	134.5	$1.99\cdot10^9$	132.,1
1199 [N]	$2.07\cdot10^9$	145.7	$2.15\cdot10^9$	142.9

As the test is performed in an oil bath, with a friction coupling with point contact, and a "piezovasque-elastic" lubrication regime (EHD – elastohydrodynamic), it was established that the appropriate lubricant is type T90 – oil for motor vehicle transmissions with viscosity corresponding to SAE class 90, with extreme pressure additives, EP2 level.

In order to be tested for rolling contact fatigue, the samples were sanded with abrasive paper of different granulation and polished with diamond solution to reduce the surface roughness, the initial and final values being presented in TABLE 3. After this, the samples were coupled with uncovered samples from the same substrate, being applied tests to batches of three samples of each type.

TABLE 3

Mean roughness of the samples

Mean roughness / Sample	P1	P2
as sprayed	9.1842 μm	4.1417 μm
finished	0.1126 μm	0.709 μm

The test cycle was set for 54 hours of test rig operation, so 4.47 [mil.rot] for an engine speed of 1380 rpm. For the calculation of the number of cycles, we took into account the fact that we are dealing with the configuration of an axial bearing with 13 balls (u = Z • 0.5 = 6.5, Z – number of balls, u – number of stresses per rotation) [19,20], so the tests were performed for 29.63 [million cycles].

3. Results and discussions

3.1. Thermal coatings characterisation

The morphology of the coatings was analyzed by electron microscopy on fracture of the layer, as shown in Fig. 5a and b.

It is observed, in both cases, the specific lamellar layered aspect of the coatings made by thermal spraying, in accordance with the results available in the literature [21,22]. However, there are differences caused by the crystallization of the splats specific to each material. Thus, it is observed in the case of the coating produced from Ni-Al-Mo (shown in Fig. 5a) the well-defined lenticular aspect and the stratification of the splats, but a lower cohesion between them (the empty spaces left between some of the splats are observed). Also visible is the columnar appearance of the splats produced during the solidification process.

Fig. 5b shows the fracture aspect in the case of the Al_2O_3-TiO_2 coating. The layer is also characterized by the lenticular structure specific to the layers deposited by atmospheric plasma spray. It is highlighted that the splats have a smaller structure in terms of size compared to the structure of the Ni-Al-Mo layer. In contrast, even if the splats can be seen well defined after breaking, those areas of lack of adhesion between them are not observed, the layer being much more compact and homogeneous.

Also with the help of electron microscopy, measurements of the deposited layer were performed, being determined the thicknesses of the layers, with values between 50-90 μm, as can be seen in Fig. 6a, b.

The structural observations are completed by the analysis of the existing phases and constituents in the powder and in the coatings, the characteristic X-ray diffraction patterns being presented in Figs 7 and 8.

Fig. 7 shows the X-ray diffraction pattern of Ni-Al-Mo powder used for plasma jet coating and of the layer obtained from this process. The powder pattern shows the presence of the elements Ni, Al and Mo, while the one of the coating indicates some intermetallic compounds resulted from the plasma spray process: NiAl, Al_3Ni_2, MoNi δ phase. This demonstrates that dur-
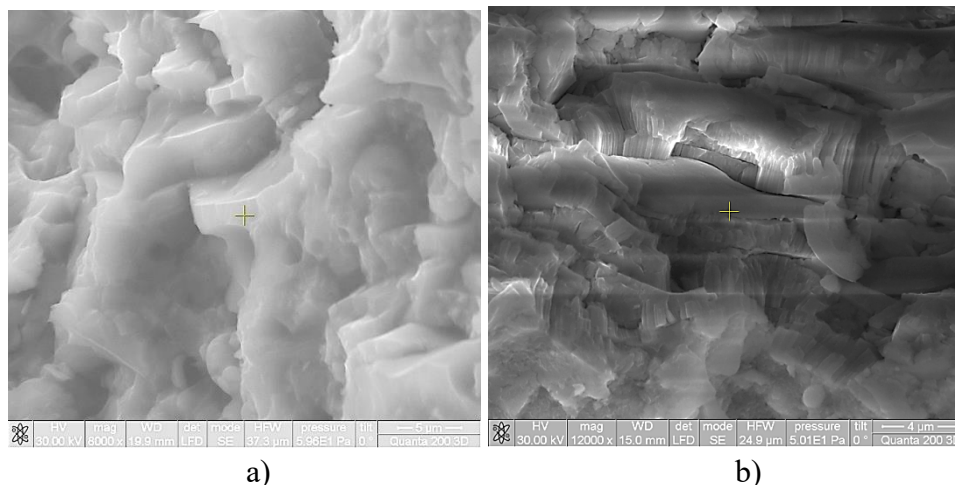

a)   b)

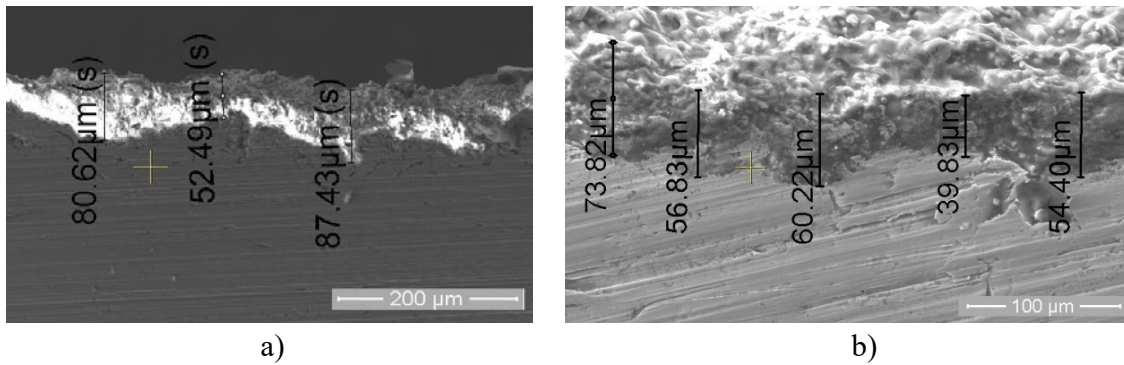Fig. 5. SE fracture images in case of samples: a) P1 (8.000×), b) P2 (12.000×)

Fig. 6. SE images of the cross-section of samples: a) P1; b) P2

ing the spraying process, even if there are phenomena that occur at very high speeds and in a very short time (milliseconds) there are reactions that occur between the molten elements accelerated in the plasma jet [23,24]. It is possible that these reactions continue when the molten particles have reached the substrate, so that the contact area has undergone a local melting under the influence of high temperature during the process, creating the

premises for the formation of metallurgical bonds between the layer thus deposited and substrate.

The XRD analysis (Fig. 8) of the powder used to obtain the P2 sample highlighted its composition: αAl_2O_3 (corundum) and γAl_2O_3 in approximately equal proportions, TiO_2 (both in the form of anatase and rutile). The general crystalline composition of the sprayed ceramic layer shows that most of the crystal-
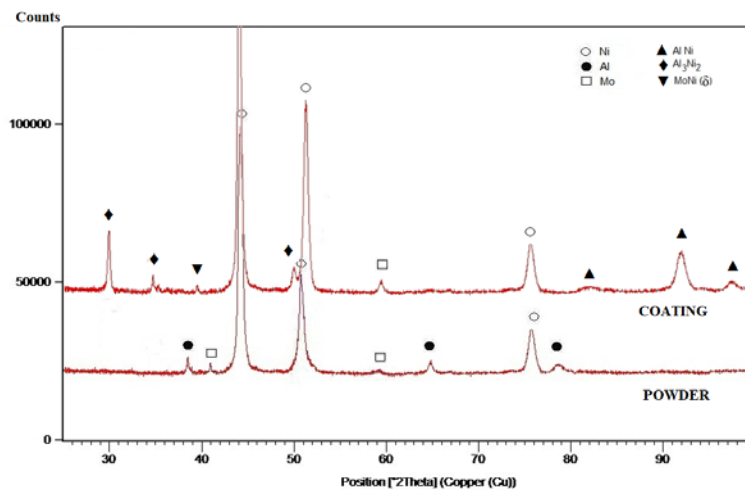

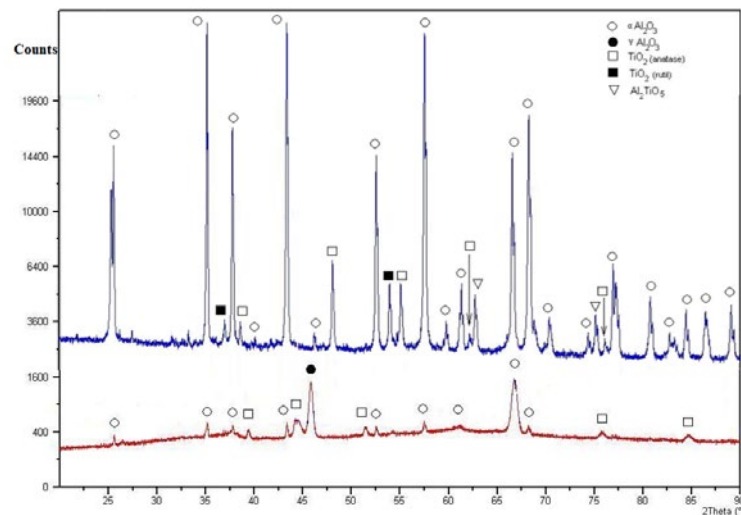Fig. 7. X-ray diffraction patterns of the Ni-Al-Mo powder and coating (sample P1)

Fig. 8. X-ray diffraction patterns of the Al_2O_3-TiO_2 powder and coating (sample P2)

line phases are: α Al_2O_3 (corundum); TiO_2 (both in the form of anatase – mostly and rutile), but also a newly formed phase – Al_2TiO_5 – a complex chemical compound. The high proportion of α Al_2O_3 can be explained considering that during the deposition process the powder is melted in the plasma jet with the formation of the γ Al_2O_3 phase, but as the particles reach the substrate they cool at a sufficiently low speed (due to substrate heating), which allows the transformation of the entire amount of γ Al_2O_3 into α Al_2O_3 [25,26].

3.2. Rolling contact fatigue behaviour

At the end of each test cycle, the samples were disassembled, cleaned in an ultrasonic bath and analyzed using a stereomicroscope at magnifications between 10×-40×, in order to make an initial evaluation of the results, as shown in Figs 9 and 10. For each case, the general appearance of both the tested ring and the bearing balls used for the respective test was highlighted, as well as the appearance of the wear path resulting from the contact fatigue test.

In the case of the samples on which the NiAlMo layers were deposited, (see Fig. 9a, c) it is observed the appearance of a wear path following the fatigue tests, in this case being obvious the damage to a greater extent of the coating. This aspect results

from the large width of the wear path (≈1 mm) and from the appearance of wear spots on the surface of some of the bearing balls, as presented in Fig. 9b.

In the case of the ceramic layer (P2) the appearance of the wear path (see Fig. 10a, c) is observed, which is much less obvious than in the previous case, having a much smaller width (≪1 mm). Also, no stains or scratches are observed on the bearing balls used for the tests, as presented in Fig. 10b.

A sample was taken from each set for analysis by electron microscopy of the morphology of the surfaces of the wear paths generated after the tests, as presented in Figs 11 and 12.

It is observed, in the case of P1 coating, the formation of a wear path with a width between 700 μm – 1 mm and the high porosity aspect, seeming to have occurred as a result of a "rolling" phenomenon during the contact fatigue test cycle, followed by a removal of the deposited layer by "pushing" it towards the edges of the tread. This hypothesis was considered because no obvious edge of exfoliation of the layer was observed in the wear path area. All samples from the P1 set had a similar behavior to contact fatigue: the coating was affected and failed following these tests. This aspect is highlighted with the help of elemental chemical analyzes of EDS type whose result is presented in Fig. 13: the presence of the element Fe on the distribution map of the analyzed area, only on the wear path width, represents the removal of the NiAlMo coating.
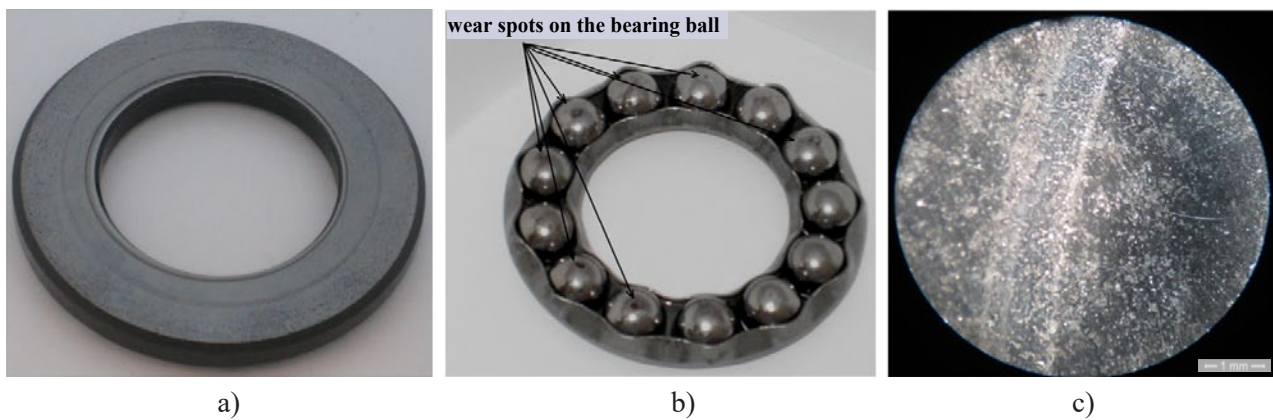

wear spots on the bearing ball

a)   b)   c)

Fig. 9. Sample P1 appeareance of: a) the ring surface after the test; b) the bearing balls used at the test; c) the resulted wear path
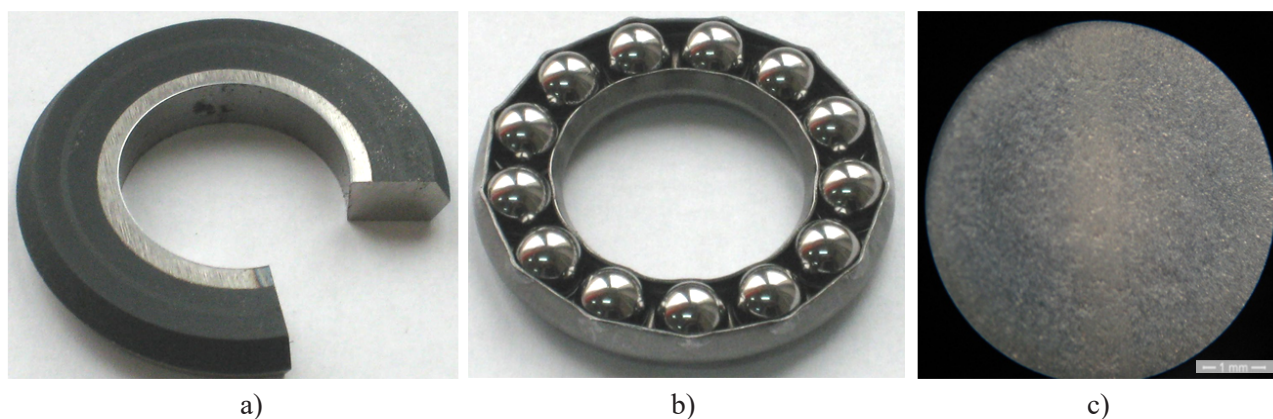

a)   b)   c)

Fig. 10. Sample P2 appeareance of: a) the ring surface after the test; b) the bearing balls used at the test; c) the resulted wear path
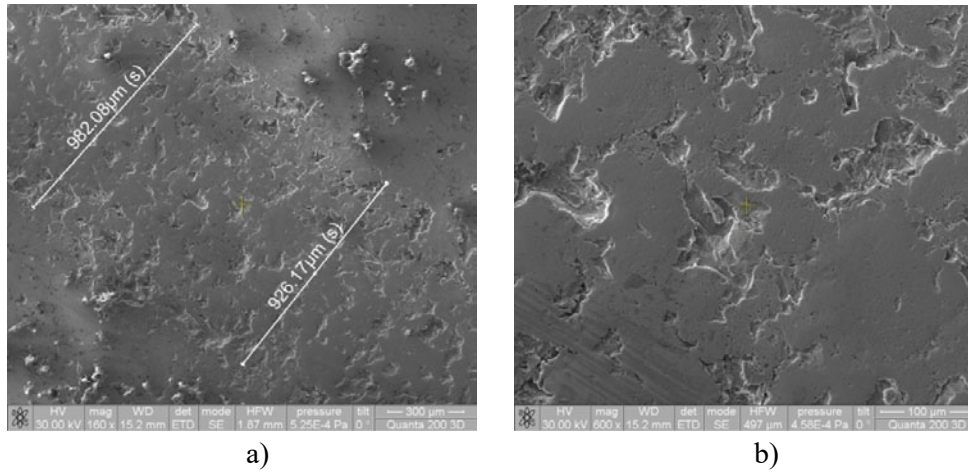
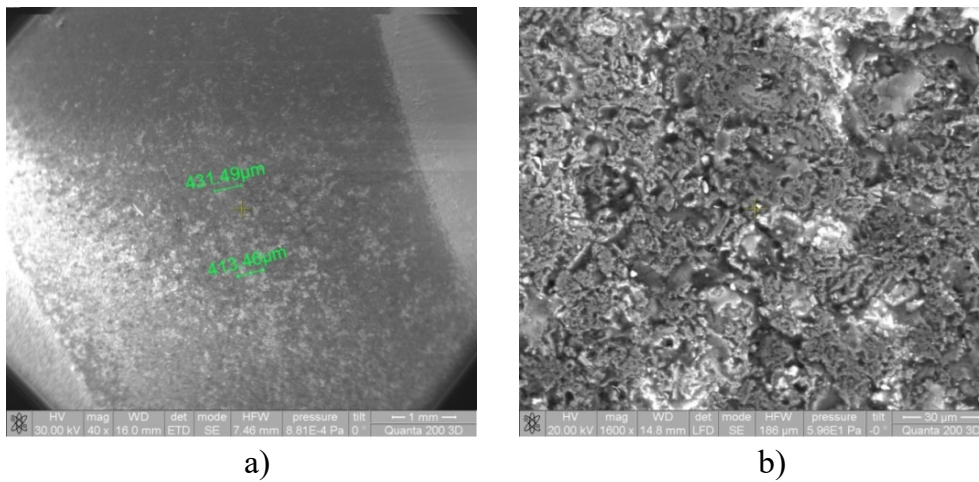Fig. 11. Appearance and dimension of the wear path in case of the sample P1: a) 160×; b) 600×

Fig. 12. Appearance and dimension of the wear path in case of the sample P2. a) 40×; b) 1600×

In the case of the samples obtained by Al_2O_3-TiO_2 it is observed that the width of the wear path is between 300 µm-450 µm, but with very few changes in the surface morphology of the layer, as can be seen in Fig. 12. The fact that no exfoliation of the coating was produced is demonstrated by the elemental chemical analysis of EDS type shown in Fig. 14, which shows only the presence of Al, O, and Ti in the analyzed area, as well as by the map in Fig. 15 which shows the uniform distribution of those chemical elements.

In order to appreciate the wear of the layers deposited on the two types of samples, measurements of the wear path produced after the rolling contact fatigue test were performed.

These measurements were conducted using the Form Talysurf Intra system, by passing the sample in transverse directions on the wear path, in Fig. 16a, b being presented the profiles resulted on a representative area of each of the samples.

The profile of the wear path produced in the case of P1 samples (Fig. 16a) supports the observations made previously, according to which a removal of the coating material was produced as a result of rolling contact fatigue tests. In the case of P2 samples there was no obvious change in depth in the contact area of the ring surface, as shown in the profile in Fig. 16b, but only a small change in roughness from Ra = 0.709 µm to Ra = 0.98 µm.

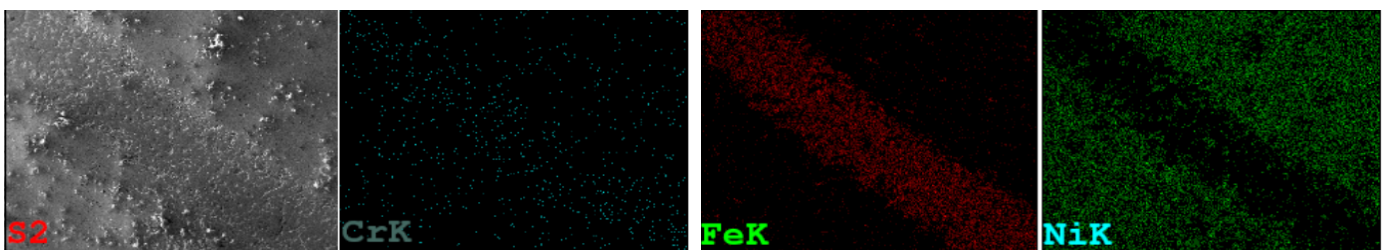Fig. 13. Chemical elements distribution map on the wear path of sample P1

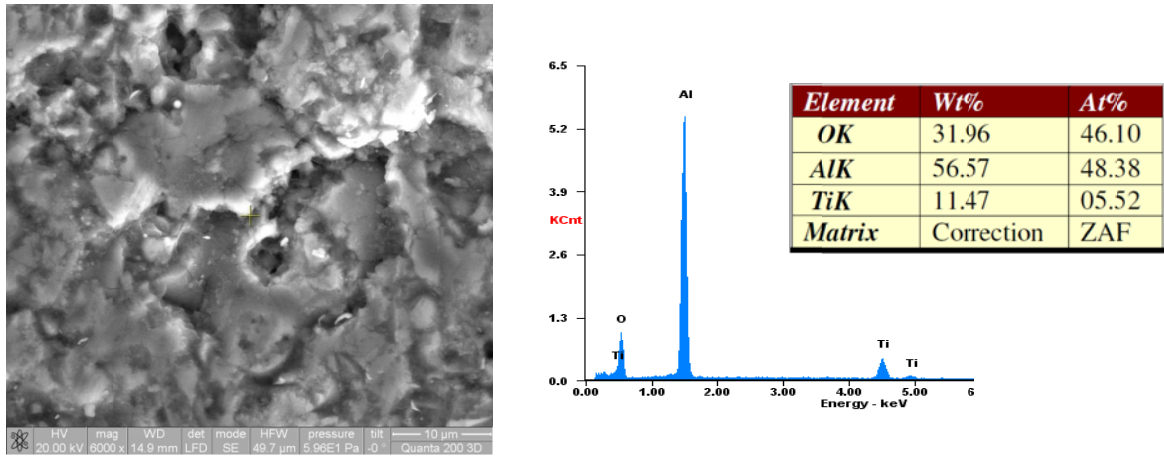| Element	Wt%	At%
OK	31.96	46.10
AlK	56.57	48.38
TiK	11.47	05.52
Matrix	Correction	ZAF

Fig. 14. The SE image of the wear path in case of sample P2 (6000×), and the EDS spectrum of the entire surface
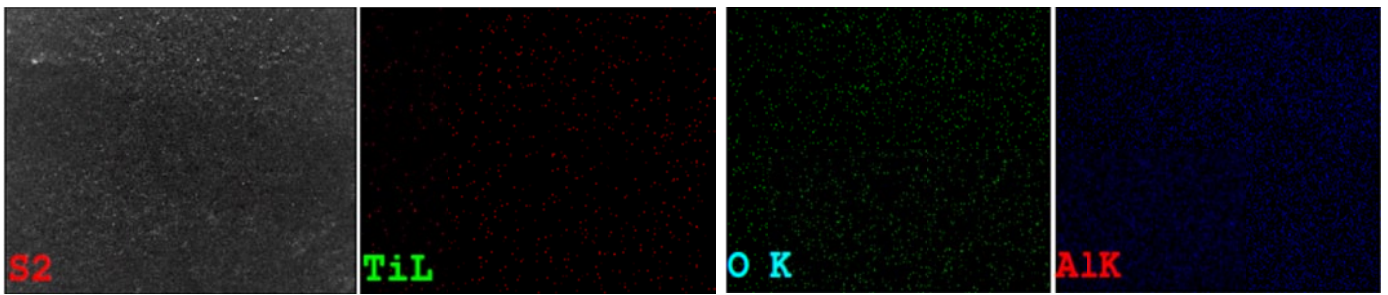

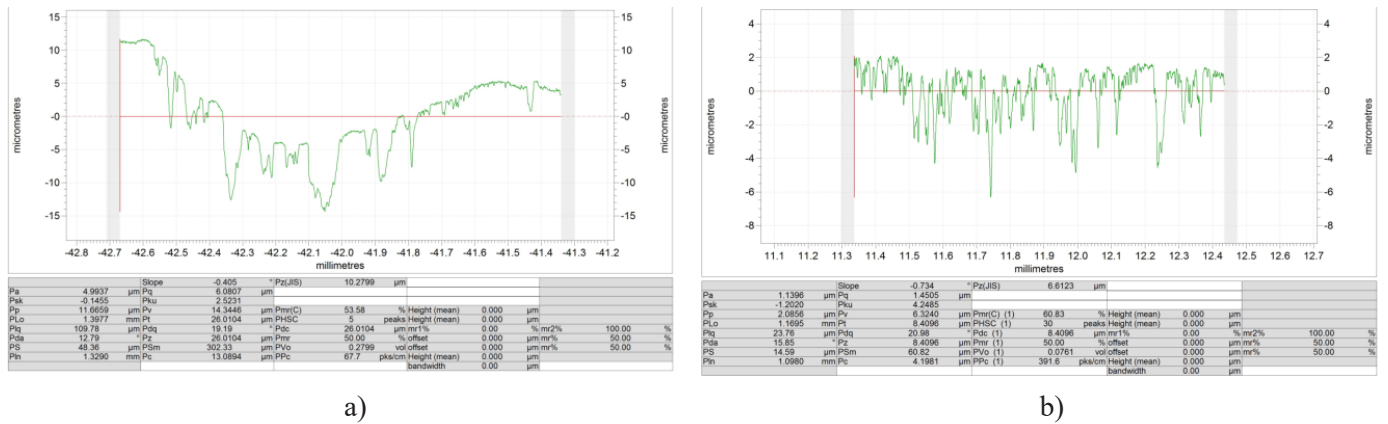Fig. 15. Chemical elements distribution map on the wear path of sample P2

a)

b)

Fig. 16. Wear path profile, in case of sample: a) P1, b) P2

4. Conclusions

The rolling contact fatigue test was performed on a test rigspecially designed for tests of this type of classic bearings. The samples were tested and the results were evaluated by direct observation (using a stereomicroscope and electron microscope), by elemental chemical analysis (EDS type) and by measuring the profiles and roughness of the areas subjected to this test.

In the secondary electron images of the layers before testing, the lamellar structure of the coatings was highlighted, more pronounced for P1 type (which negatively influences the cohesion of the coating and the behavior at mechanical stress) and very little visible in P2 case (characterized by a crystallization of particles with much smaller dimensions and various geometries, which positively influences the behavior at the stresses characteristic for the bearings).

By the X-ray diffraction analysis performed on the powders and on the coatings obtained from them, it was observed the appearance of new phases (type Al_2TiO_5 in case of P2) and intermetallic compounds (AlNi, Al_3Ni_2, MoNi in case of P1) whose presence influences differently the behavior of the layers at stress and gives indications about the physico-chemical phenomena produced during the spraying.

Following the contact fatigue test, it was observed that the P2 sample had an appropriate behavior, characterized by the appearance of slight traces of abrasion and spalling wear (in some places), unlike the P1 sample, for which the deposited layer was completely removed.

In both cases, the appearance of a wear path was observed, which was much more obvious in the case of the Ni matrix layer, predominantly caused by the plastic deformation of the coating, produced by pushing the material towards the edges of the wear path. In the case of the ceramic coating, the width of the wear path was very small (300-450 μm), with very few changes at the surface level of the coating, which recommends this type of material for applications that require wear resistance to rolling.

A correlation can be made between the results and the microstructural characteristics (the way of coating formation and the geometry of the splats) and those of the material (modulus of elasticity and hardness), there being a direct dependence between them and the performances of the layers: the layers with a less obvious lamellar geometry withstood better, these being also those characterized by a higher hardness and modulus of elasticity, recommended for the realization of some coatings that will successfully respond to the rolling contact type stresses.

REFERENCES

[1] J.R. Davis (Ed.), Handbook of thermal spray technology, ASM International, Materials Park, OH, USA, 2004.

[2] L. Pawlowski (Ed.) 1995 The Science and Engineering of Thermal Spray Coatings, John Wiley & Sons Ltd, New York.

[3] D. Chicet, A. Tufescu, C. Paulin, M. Panturu, C. Munteanu, The Simulation of Point Contact Stress State for APS Coatings, IOP Conference Series: Materials Science and Engineering **209** (1), art. no. 012044, (2017).

[4] D.B. Bitanu et al., IOP Conf. Ser.: Mater. Sci. Eng. **133**, 012031 (2016).

[5] D.C. Achitei, Abdullah Mohd Mustafa Al Bakri, A.V. Sandu, C.A. Tugui, M. Benchea, IOP Conf. Ser.: Mater. Sci. Eng. **209**, 012053 (2017).

[6] R. Suryanarayanan, Plasma spraying: theory and applications, published by World Scientific Publishnig, Singapore, 1993, ISBN 981-02-1363-8.

[7] C. Paulin, D.L. Chicet, B. Istrate, M. Panturu, C. Munteanu, IOP Conference Series: Materials Science and Engineering **147**, 012034 (2016).

[8] P. Avram, M.S. Imbrea, B. Istrate, S.I. Strugaru, M. Benchea, C. Munteanu, Indian Journal of Engineering and Materials Sciences **21** (3) 315 (2014).

[9] M. Panturu, D. Chicet, S. Lupescu, B. Istrate, C. Munteanu, Acta Technica Napocensis Series-Applied Mathematics Mechanics And Engineering **61**, 137 (2018).

[10] P. Vuoristo, Thermal Spray Coating Processes, Comprehensive Materials Processing **4**, 229-276 (2014).

[11] S. Lupescu, C. Munteanu, A. Tufescu, B. Istrate, N. Basescu, Contact stress simulation **997**, 1, Article number 012024 (2020).

[12] M.R. Balan, A. Tufescu, S.S. Cretu, A case study on relation between roughness, lubrication and fatigue life of rolling bearings, IOP Conference Series: Materials Science and Engineering **147**, 1, Article number 012013 (2016).

[13] A. Tufescu, S. Cretu, M.R. Balan, The role of roughness amplitude on depth distribution of contact stresses, IOP Conference Series: Materials Science and Engineering **147**, 1, Article number 012012 (2016).

[14] D. Olaru, Fundamente de lubrificaţie (Lubrication fundaments), Ed. "Gh. Asachi" Iaşi, 2002.

[15] Sp. Creţu, Mecanica contactului (Contact mechanics), Ed. "Gh. Asachi" Iaşi, 2002.

[16] P. Niranatlumpong, H. Koiprasert, The effect of Mo content in plasma-sprayed Mo-NiCrBSi coating on the tribological behavior, Surface & Coatings Technology **205**, 483-489 (2010).

[17] S. Cretu, Ghe. Constantin, S. Grigoras, Ghe. Iliescu, T. Nestor, Masina pentru incercari la oboseala, brevet inventie nr. 87308/1985.

[18] G. Stachowiak, A. W. Batchelor, Engineering Tribology, 3rd Edition, 2005, published by Butterworth-Heinemann, eBook ISBN: 9780080531038.

[19] M. Gafitanu, D. Nastase, Sp. Cretu, Gh. Coman, C. Racocea, T. Nestor, D. Olaru, Rulmenti. Proiectare si tehnologie, vol II, Editura Tehnica, Bucuresti, 1985.

[20] M. Gafitanu, D. Nastase, Sp. Cretu, D. Olaru, Rulment. Proiectare si tehnologie, vol. I, Editura Tehnica, Bucuresti, 1985.

[21] C.C. Paleu, C. Munteanu, B. Istrate, S. Bhaumik, P. Vizureanu, M.S. Bălţatu, V. Paleu, Microstructural Analysis and Tribological Behavior of AMDRY 1371 (Mo-NiCrFeBSiC) Atmospheric Plasma Spray Deposited Thin Coatings, Coatings **10** (12), 1186 (2020).

[22] M. Lutcanu, B. Istrate, M. Coteata, D.L. Chicet, I. Ionita, C. Paraschiv, I. Stirbu, G. Badarau, N. Cimpoesu, Structural aspects and chemical analyses on cutting process of metallic-ceramic materials, IOP Conference Series: Materials Science and Engineering **1037**, 1, Article number 012033 (2021).

[23] Piao Zhong-yu, Xu Bin-shi, Wang Hai-dou, Pu Chun-Huan, Investigation of rolling contact fatigue lives of Fe-Cr alloy coatings under different loading conditions, Surface & Coatings Technology **204**, 1405-1411 (2010).

[24] Zhongyu Piao, BinshiXu, HaidouWang, Chunhuan Pu, Influence of undercoating on rolling contact fatigue performance of Fe-based coating, Tribology International **43**, 252-258 (2010).

[25] E. Sanchez, E. Bannier, V. Cantavella, M.D. Salvador, E. Klyatskina, J. Morgiel, J. Grzonka, A.R. Boccaccini, Deposition of Al2O3-TiO2 Nanostructured Powders by Atmospheric Plasma Spraying, JTTEE5 **17**, 329-337 (2008).

[26] LI Chang-qing, MA Shi-ning, YE Xiong-lin, Tribological properties of nanostructured n-Al2Os/Ni coatings deposited by plasma spraying **12** Suppl 2 J. Cent. South Univ. Technol. Article ID: 1005-9784 (2005).